MASTER COPY FOR REPRODUCTION PURPOSES

REPORT DOCUMENTATION PAGE

1a. REPORT SECURITY CLASSIFICATION Unclassified	1b. RESTRICTIVE MARKINGS
2a. SECURITY CLASSIFICATION AUTHORITY	3. DISTRIBUTION/AVAILABILITY OF REPORT Approved for public release; distribution unlimited.
AD-A213 507 (S)	5. MONITORING ORGANIZATION REPORT NUMBER(S) ARO 22306.13-EG
6a. NAME OF PERFORMING ORGANIZATION Brown University 6b. OFFICE SYMBOL (If applicable)	7a. NAME OF MONITORING ORGANIZATION U. S. Army Research Office
6c. ADDRESS (City, State, and ZIP Code) Brown University Providence, RI 02912	7b. ADDRESS (City, State, and ZIP Code) P. O. Box 12211 Research Triangle Park, NC 27709-2211
8a. NAME OF FUNDING/SPONSORING ORGANIZATION U. S. Army Research Office 8b. OFFICE SYMBOL (If applicable)	9. PROCUREMENT INSTRUMENT IDENTIFICATION NUMBER DAAG29-85-K-0003
8c. ADDRESS (City, State, and ZIP Code) P. O. Box 12211 Research Triangle Park, NC 27709-2211	10. SOURCE OF FUNDING NUMBERS PROGRAM ELEMENT NO. / PROJECT NO. / TASK NO. / WORK UNIT ACCESSION NO.

11. TITLE (Include Security Classification)
Micromechanisms of Dynamic Crack Propagation in an AISI 4340 Steel

12. PERSONAL AUTHOR(S)
Rodney J. Clifton

13a. TYPE OF REPORT	13b. TIME COVERED	14. DATE OF REPORT (Year, Month, Day)	15. PAGE COUNT
Reprint	FROM ____ TO ____		

16. SUPPLEMENTARY NOTATION
The view, opinions and/or findings contained in this report are those of the author(s) and should not be construed as an official Department of the Army position, policy, or decision, unless so designated by other documentation.

17. COSATI CODES		
FIELD	GROUP	SUB-GROUP

18. SUBJECT TERMS (Continue on reverse if necessary and identify by block number)

19. ABSTRACT (Continue on reverse if necessary and identify by block number)

ABSTRACT ON REPRINT

20. DISTRIBUTION/AVAILABILITY OF ABSTRACT	21. ABSTRACT SECURITY CLASSIFICATION
☐ UNCLASSIFIED/UNLIMITED ☐ SAME AS RPT. ☐ DTIC USERS	Unclassified
22a. NAME OF RESPONSIBLE INDIVIDUAL	22b. TELEPHONE (Include Area Code) / 22c. OFFICE SYMBOL

DD FORM 1473, 84 MAR 83 APR edition may be used until exhausted. All other editions are obsolete.

Materials Science and Engineering, A112 (1989) 79–88

Micromechanisms of Dynamic Crack Propagation in an AISI 4340 Steel

R. GODSE*, G. RAVICHANDRAN† and R. J. CLIFTON

Division of Engineering, Brown University, Providence, RI 02912 (U.S.A.)

Received July 18, 1988; in revised form November 10, 1988

Abstract

The present work is aimed at understanding the micromechanisms of dynamic crack growth at room temperature and a low temperature (−100 °C) in an AISI 4340 steel studied by Ravichandran and Clifton. For this purpose, a fractographic and metallographic examination of the specimens used by Ravichandran and Clifton was carried out. Results showed that the steel contained an appreciable amount of upper bainite (about 15%). The study suggests that dynamic crack propagation in the 4340 steel occurs in two stages, i.e. nucleation of microcracks in the upper bainite followed by propagation of these microcracks into the surrounding martensite. At low temperatures, failure of the martensite occurs by cleavage whereas, at room temperature, it occurs by shear localization, leading to microvoid growth and coalescence. At both temperatures, bainitic microcracks serve as failure initiation sites and reduce the dynamic fracture toughness of the steel.

1. Background

Recently, Ravichandran and Clifton [1] have developed a new plate impact experiment for studying fracture under very high loading rates. The experiment consists of impacting a precracked disc-shaped specimen by a thin flyer plate (Fig. 1). On impact, a compressive pulse travels through the specimen and reflects from the rear surface as a step tensile pulse which loads the crack and causes it to advance over a distance determined by the amplitude and duration of the tensile pulse. Initiation of the crack advance occurs within a few hundred nanoseconds of the arrival of the tensile pulse at the crack front. As a result, the loading rates achieved in this technique are of the order of 10^6 MPa $m^{1/2}$ s^{-1}—approximately two orders of magnitude higher than those obtained in other techniques. The plate impact method thus makes it possible to study the fracture resistance of materials under conditions of extremely rapid loading.

By using the plate impact technique, Ravichandran and Clifton [1] studied dynamic crack propagation in a hardened AISI 4340 VAR steel at −100 and −80 °C (low temperature experiments) and at room temperature. From experimentally measured distances of crack advance, they calculated the critical value K_{Ic} of the stress intensity factor by using known elastodynamic solutions to the crack propagation problem. They computed a K_{Ic} value of 32 MPa $m^{1/2}$ for the low temperature experiments and 62 MPa $m^{1/2}$ for the room temperature experiments. After preliminary fractographic examination, they con-

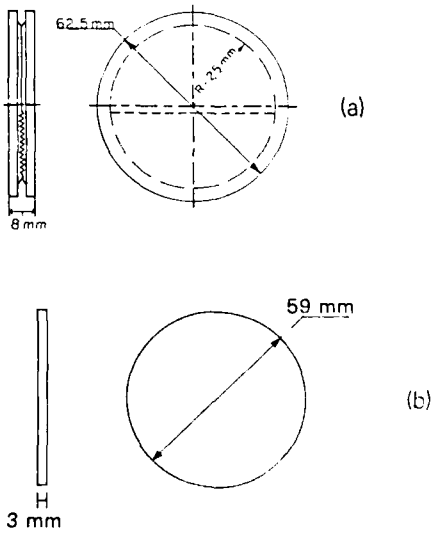

Fig. 1. Geometry of (a) the plate impact specimen and (b) the flyer plate.

*Present address: Philip McKenna Laboratory, Kennametal Inc., P.O. Box 639, Greensberg, PA 15601, U.S.A.

†Present address: Department of Applied Mechanics, University of California at San Diego, Lajolla, CA 92093, U.S.A.

0921-5093/89/$3.50

cluded that dynamic fracture in the 4340 steel studied occurs at low temperatures predominantly by cleavage, whereas at room temperature it occurs in a ductile manner characterized by void growth and coalescence.

The present work was undertaken to gain an improved understanding of the micromechanisms of crack growth and the role played by the microstructure in dynamic fracture at the very high loading rates attained in the plate impact experiments. For this purpose, the 4340 steel specimens used by Ravichandran and Clifton in their plate impact experiments were studied in greater detail. In particular, crack tip–microstructure interactions were studied by examining the fracture surfaces and the crack profiles by scanning electron microscopy. Specimens impacted at both low and room temperatures were studied in this manner.

A large number of studies have focused on the fracture mechanisms in 4340 steels under quasi-static loading. Various aspects of the failure characteristics of these steels, such as the effect of microstructure, austenitizing temperature, test temperature and processing history on the mechanical properties including fracture toughness, tensile strength, ductility and Charpy impact energy, are well documented. These studies have been summarized in the recent works of Lee *et al.* [2] and Tomita [3]. On the contrary, studies related to crack growth mechanisms in 4340 steels under dynamic loading are limited in number. Chi *et al.* [4] have measured the quasi-static and dynamic fracture toughness of a 4340 steel and have conducted a fractographic and metallographic study of their specimens. Their work is discussed later in the present paper.

The experimental procedure used by Ravichandran and Clifton is summarized below. The composition of the 4340 steel is given in Table 1. The fatigue specimen (Fig. 2(a)) was machined from an ingot bar, 62.5 mm in diameter, obtained in the as-rolled condition. The specimen was austenitized at 870 °C for 2 h, quenched in agitated oil and subsequently tempered at 100 °C for 2 h. It was found that, owing to the relatively large size of the fatigue specimen, the steel had not fully hardened throughout the cross-section. Rockwell C hardness measurements indicated that the hardness varied from 52 HRC at the center to 57 HRC at the circumference of the specimen.

The heat-treated fatigue specimen was subjected to cyclic bending in a four-point bend configuration (Fig. 2(b)). After obtaining the required amount of fatigue crack growth (half-way across the diameter), the fatigue specimen was unloaded. The plate impact specimen shown in Fig. 1(a) was then machined from the fatigue specimen and used for a dynamic crack growth study. Following the plate impact experiment, selected specimens were "opened" by wedge loading in liquid nitrogen. These specimens were used for fracture surface examination.

2. Experimental procedure

In the present work, samples for microstructural examinations were sectioned from various

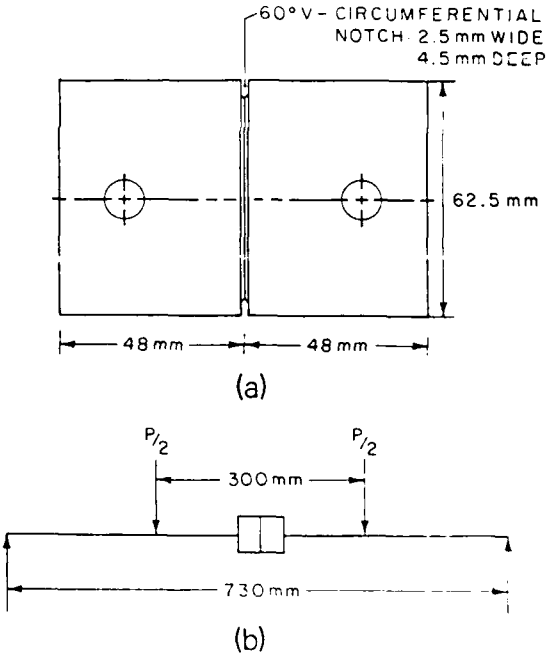

Fig. 2. Schematic diagrams of (a) the fatigue specimen and (b) the fatigue loading configuration.

TABLE 1 Chemical composition of 4340 VAR steel (Republic Steel: heat 3841687)

Element	C	Mn	Ni	Cr	Mo	Cu	Si	Al	P	S	N	O	H
Amount wt%	0.42	0.46	1.74	0.89	0.21	0.28	0.19	0.031	0.009	0.001	0.005	0.001	1.0 wt ppm

Heat treatment: austenitize at 870 °C for 2 h, oil quench; temper at 100 °C for 2 h, air cool.
Hardness: 52 HRC

locations along the radius of the plate impact specimen. These samples were polished metallographically, etched to reveal the prior austenite grain boundaries and examined in an optical microscope. The etchant used for this purpose was a saturated aqueous solution of picric acid with a small addition of sodium tridecyl benzene sulfate which acts as a wetting agent. The samples were then repolished and etched to reveal the presence of bainite. The etchant was a solution of 1 g of sodium bisulfate and 4 g of picric acid in 100 ml of water and 100 ml of ethyl alcohol.

Selected (unopened) plate impact specimens were sectioned to obtain samples containing mid-thickness profiles of dynamically grown cracks. The sectioned samples were ground, polished and examined in an AMR-1000A scanning electron microscope in the following manner.

(a) In order to study the relation between the fracture path and the prior austenite grain boundaries, crack profiles were studied in two stages. Initially the crack profiles were photographed in an unetched condition. The samples were then etched to reveal the prior austenite grain boundaries and re-examined. By this two-stage procedure, it was possible to distinguish clearly between crack-like features and grain boundaries.

(b) To study the relation between the crack path and the microstructural constituents, the samples were repolished and etched to reveal bainite. This part of the examination was repeated three times to check the consistency of the results.

Fracture surfaces of opened specimens were studied in the unetched and etched conditions. Both halves of the opened specimens were examined to obtain a clear picture of the topography of mating surfaces.

3. Results

Microstructural examination of the specimen circumference showed that the steel had effectively hardened and was essentially fully martensitic, containing less than 1% bainite in that location. However, quenching rates obtained in the heat treatment of the fatigue specimens were insufficient to obtain a fully martensitic structure at the center. Quantitative measurements made on an automated image analyzer (Buehler Omnimet) showed that the volume fraction of bainite was approximately 0.15 near the center of the plate impact specimen (Fig. 3(a)). Since the carbides in the bainite have a relatively large size (Fig. 3(b)) and a stringer-like morphology (Fig. 3(c)), it can be concluded that this bainite is the so-called "upper bainite"—a microconstituent which forms isothermally at temperatures above 350 °C.

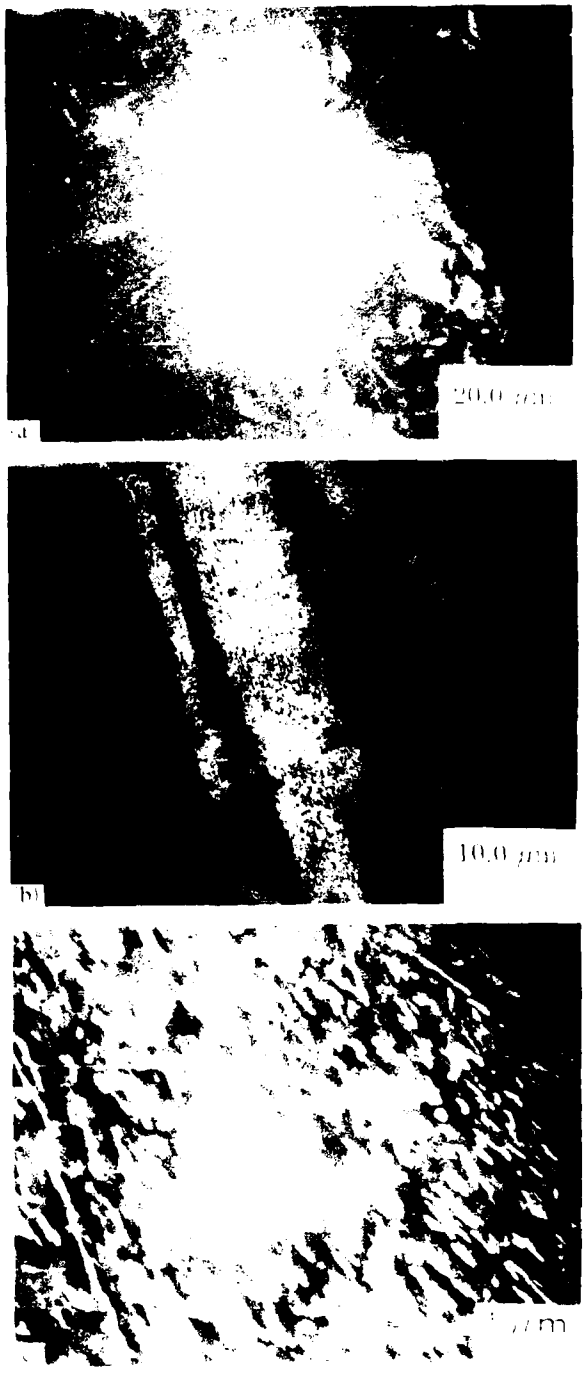

Fig. 3. Scanning electron micrographs of the microstructure of the 4340 steel: a), b) upper bainite white areas; c) carbides in bainite.

From the crack profile studies, it was found that the fracture path and the prior-austenite grain boundaries were unrelated. Crack propagation was thus transgranular with respect to the prior austenite grains. Figures 4 and 5 show the nature of the crack tip region for low temperature and room temperature experiments respectively. The total extent of the dynamic crack growth is at least three times that shown in the figures; hence the fatigue crack tip is far from the regions shown. In both cases, the crack is discontinuous near the tip and is composed of cracked segments several grain diameters long, separated by unbroken ligaments. Another important feature is the presence of small cracks with dimensions smaller than the average grain diameter (Fig. 6). Over 95% of the detected microcracks were inside bainite packets. These microcracks are either isolated from the main crack (Fig. 6(a)) or misoriented with respect to the fracture path. Figure 6(b) shows microcracks in a low temperature specimen etched to reveal prior-austenite grain boundaries, and Fig. 6(c) shows microcracks in bainite packets in a room temperature specimen. The arrows in Figs. 4–6 indicate the direction of crack propagation.

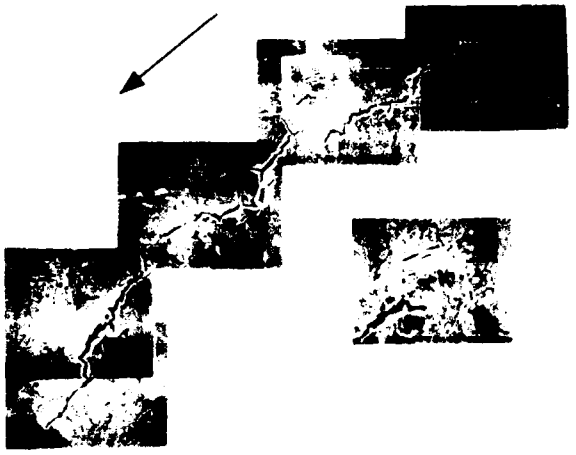

Fig. 4. Nature of the crack tip region for the low temperature experiments (shot 85-20).

Figures 7 and 8 show the fractographs of mating surfaces for the low temperature experiments. The fracture surface is composed of relatively large quasi-cleavage facets, such as that labeled QC, and numerous smaller cleavage facets. The latter are evident in the higher magnification view of Fig. 9. In addition to the cleaved regions, there are small areas, less than 5 μm in size, which consist of submicron-sized dimples. An enlarged view of one such area (labeled VS) is shown in Fig. 10. It should be noted, however, that the dimpled areas covered less than 5% of the fracture surface of the low temperature specimens. Figure 11 shows an example of the appearance of the etched fracture surfaces. The etching helps to distinguish between bainitic cleavage facets (which reveal the carbide stringers and carbide particles upon etching) and the martensitic cleavage facets. Other examples of bainitic facets on etched fracture surfaces are provided by Fig. 12.

Figure 13 shows the fractographs of mating fracture surfaces for the room temperature ex-

Fig. 5. Nature of the crack tip region for the room temperature experiments (shot 82-01).

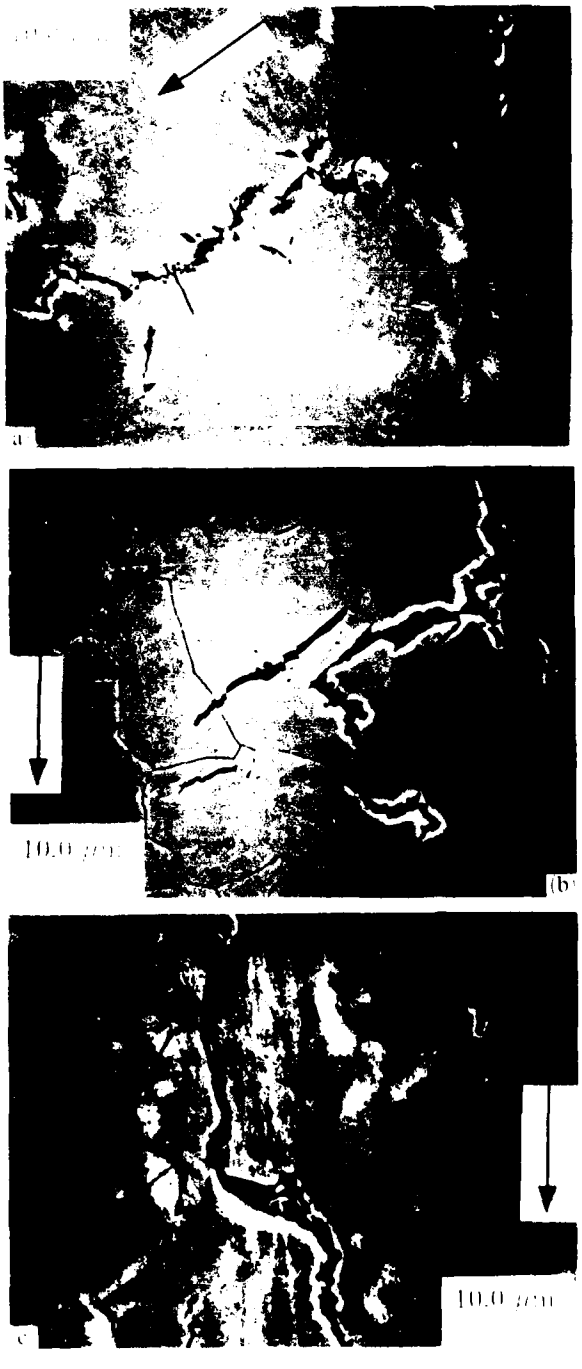

Fig. 6. Microcracks in bainite: (a) low temperature specimen (shot 85-20); (b) low temperature specimen etched to reveal prior austenite grain boundaries (shot 85-20); (c) room temperature specimen (shot 82-01).

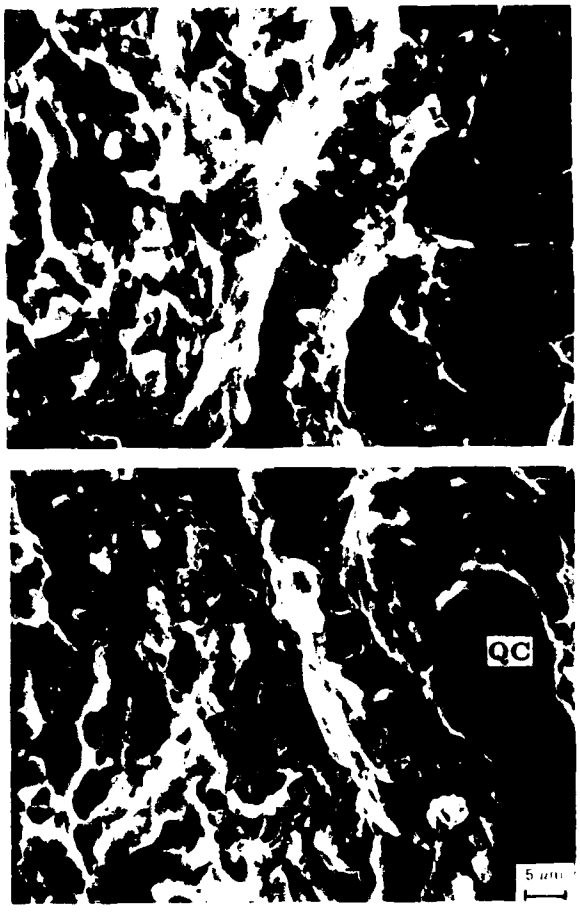

Fig. 7. Fractographs of mating surfaces for the low temperature experiment (shot 85-15).

periments. Two regions can be clearly distinguished: regions where the material fractured by cleavage (labeled QC) and regions where it failed by microvoid growth and coalescence (labeled VS). The latter regions are evident as relatively flat areas, 30 μm in size, composed of submicron-sized dimples. These areas, hereafter referred to as void sheets, are generally inclined relative to the local plane of the main crack. Figure 14 shows an enlarged view of a void sheet.

4. Discussion

The crack profile and fractographic observations discussed above allow us to deduce a probable sequence of events preceding dynamic crack propagation in the 4340 steel studied by Ravichandran and Clifton [1]. The study of crack profiles conducted in the present work has clearly shown that the primary crack is surrounded by microcracks and that an overwhelming majority of these are confined to bainitic packets. These observations suggest that dynamic fracture of the 4340 steel involves two main stages. Initially, the elevated stresses near the tip of a crack loaded by a step tensile pulse cause fracture of the bainitic

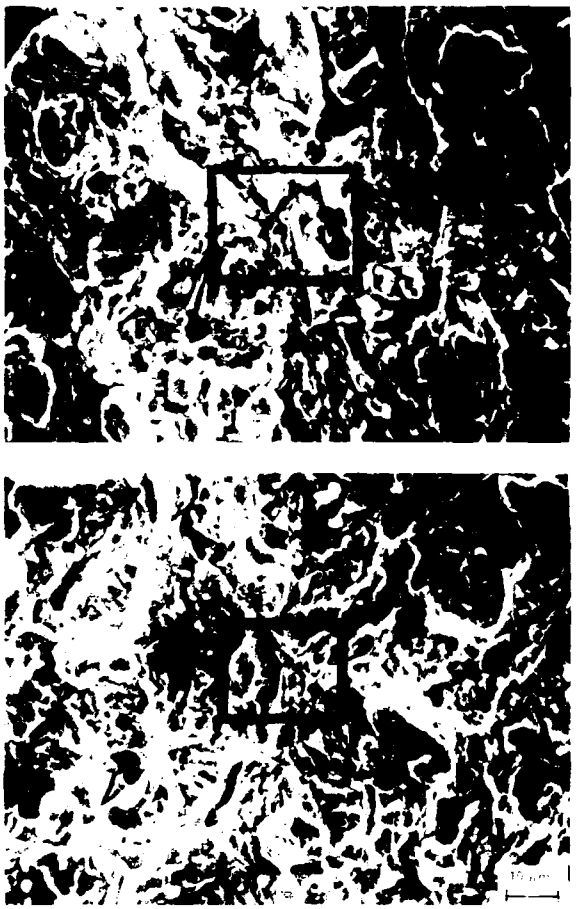

Fig. 8. Fractographs of mating surfaces for the low temperature experiment shot 85-15.

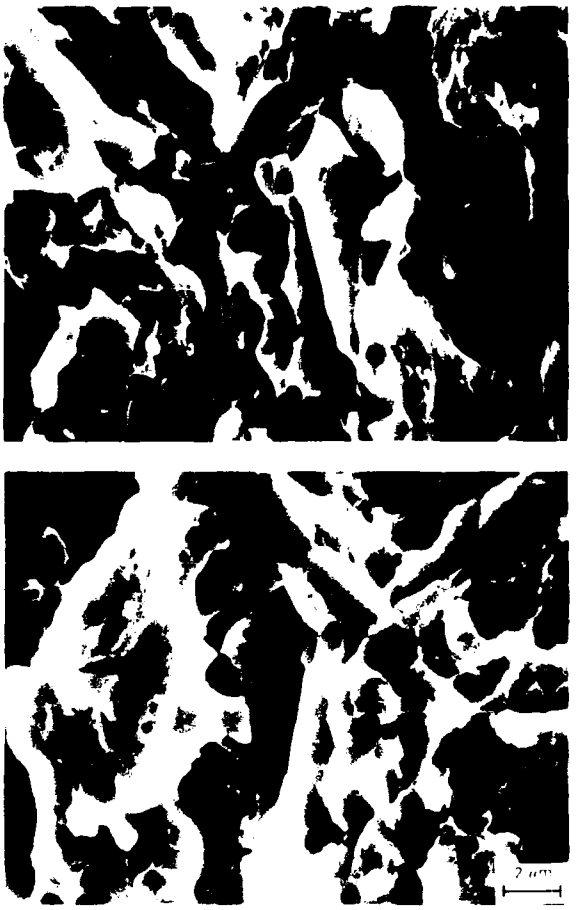

Fig. 9. Enlarged view of the areas shown in Fig. 8.

packets in the near-tip region. As indicated by the examination of the etched fracture surfaces, bainite fractures in a quasi-cleavage manner, both at low temperatures and at room temperature. This is followed by failure of the martensitic ligaments surviving between the microcracks (or between a microcrack and the crack tip). The present results suggest that the mode of martensitic fracture depends on the test temperature, as discussed below.

4.1. Low temperature fracture of martensite

The low temperature failure mechanisms in martensite under quasi-static loading are reasonably well understood [2, 3]. It is known that, under these conditions, martensite fails by cleavage along crystallographic planes in individual martensite laths and that the fracture path maintains a general direction within groups of similarly oriented laths, usually called lath packets.

Fig. 10. High magnification view of an area containing fine dimples in a low temperature specimen shot 85-15.

Owing to the difference in lath orientations between neighboring packets, the fracture path deviates at each packet boundary and the resulting fracture surface has a faceted appearance.

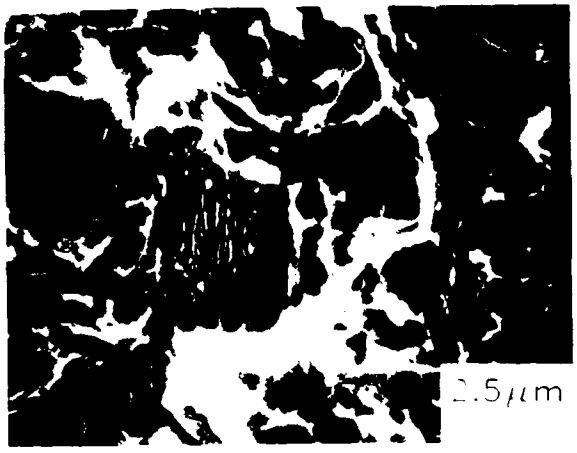

Fig. 11. Etched fracture surface showing an etched bainitic quasi-cleavage facet in a low temperature specimen (shot 85-15).

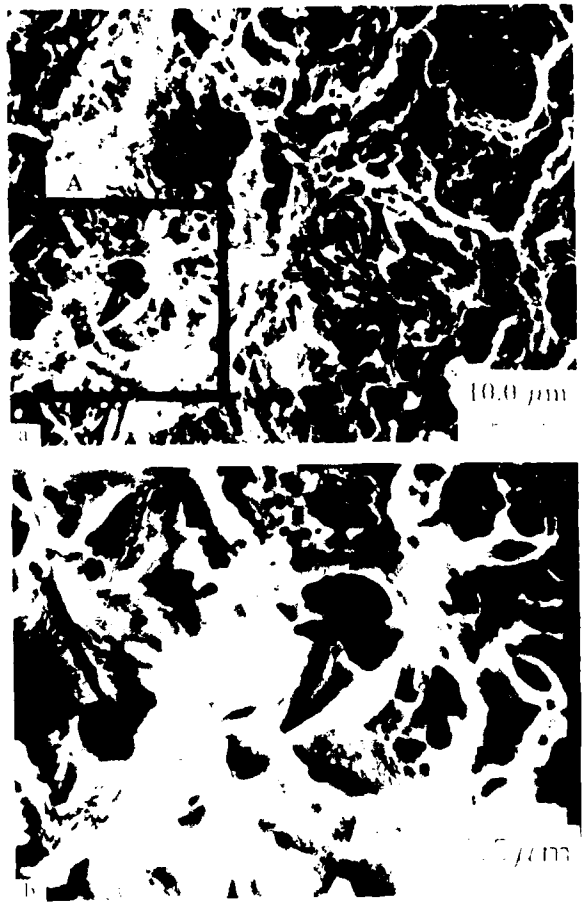

Fig. 12. (a) Appearance of the fracture surface in Fig. 8(b) after etching; (b) detail A.

These characteristic facets are called quasi-cleavage facets, since an entire facet is not produced owing to cleavage along a single crystallographic plane, as would be the case for "true" cleavage.

As shown by the fractographs in Figs. 7–9, low temperature martensitic failure under dynamic

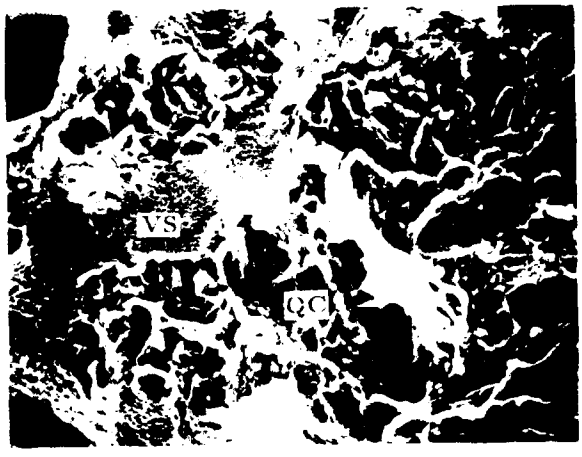

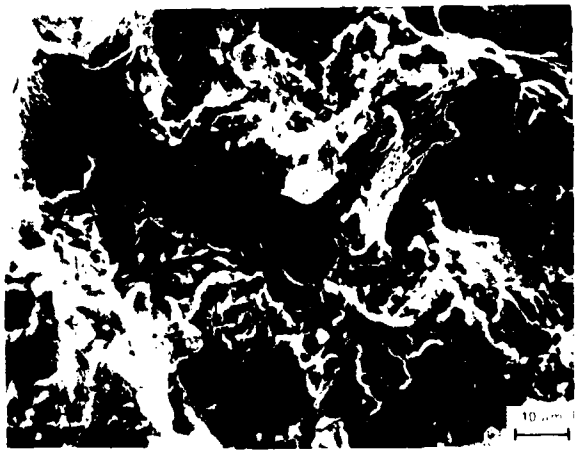

Fig. 13. Fractographs of mating surfaces for the room temperature experiment (shot 84-08).

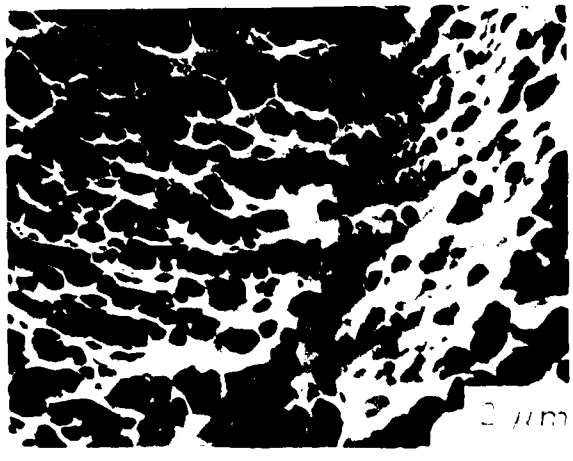

Fig. 14. Enlarged view of a void sheet (shot 84-08).

loading occurs predominantly by cleavage. The variation in the size of the quasi-cleavage facets (*e.g.* compare the facets in Fig. 7 and Fig. 9) presumably occurs owing to the variation in the lath packet size. The existence of isolated regions consisting of submicron-sized dimples, such as that labeled VS in Fig. 10, can be explained by noting that some lath packets along the fracture path in the martensitic ligaments may not be favorably oriented for cleavage. These local regions can be expected to fail at a later stage by shear localization, leading to microvoid growth and coalescence. Shear localization is discussed later in greater detail in the context of room temperature failure mechanisms.

It is interesting to note that no microcracks were detected in martensite in the crack profile studies. This suggests that cleavage fracture across a martensitic ligament between the crack tip and a bainitic microcrack probably occurs "all at once", *i.e.* the critical step governing ligament failure corresponds to the extension of a bainitic crack in the surrounding martensitic matrix.

4.2. Room temperature fracture of martensite

In the context of quasi-static fracture, it is now generally understood that localized plastic deformation leading to shear band formation in the near-tip region plays a significant role in ductile fracture processes [2, 5–12]. In particular, where ductile fracture involves void nucleation at large particles, linkage of the growing void with the crack tip may occur via shear band formation in the ligament between the growing void and the crack tip [2, 5–7]. Owing to the large strains developed within the shear band, void nucleation can take place at fine particles. Since subsequent shear band decohesion occurs by growth and coalescence of these microvoids, this mechanism of ligament failure is often called the void sheet mechanism. Under these circumstances, the fracture surface consists of dimples which fall into two distinct size groups. The larger dimples correspond to voids nucleated at large particles, such as MnS inclusions in steels, and these are surrounded by void sheets which contain the much finer dimples corresponding to the microvoids. Such bimodal dimple size distributions observed on fracture surfaces indicate that shear localization may have been operative during fracture [5, 7]. Significant efforts have been devoted towards modeling these phenomena in ductile fracture under quasi-static loading [8–11].

The occurrence of shear localization during quasi-static fracture in steels corresponding to AISI 4340 compositions has been observed by Cox and Low [12]. McMeeking [7] has suggested that such shear localization may rationalize the relatively poor quasi-static toughness of these steels. Because of the limited number of studies of dynamic fracture in 4340 steels, it is not known at present whether such effects can occur at a crack tip subjected to dynamic loading. However, fracture surfaces from Charpy impact experiments, wherein cracks grow under dynamic loading, appear to have the bimodal dimple size distribution observed for quasi-static fracture [13]. This observation suggests that shear localization may be operative under dynamic tensile loading. Furthermore, many studies have shown that shear localization does occur under dynamic shear loading [14–17].

The fractographic observations made in the present study clearly show that, for the room temperature experiments, the fracture surface consists of two distinct types of regions: regions of quasi-cleavage and regions containing fine submicron-sized dimples. The latter are present as relatively flat void sheets which link regions of quasi-cleavage and are inclined relative to the local fracture planes. On the basis of these observations, it can be postulated that, for the particular microstructure considered (martensite + upper bainite), microcracks formed in bainite during the initial loading stage link up by the growth and coalescence of microvoids within shear bands formed in the martensitic ligaments. The results of the present work thus suggest that localized plastic deformation may play as important a role in dynamic fracture as in quasi-static fracture.

Chi *et al.* [4] have measured the fracture toughness of a 4340 steel under quasi-static and dynamic loading. The dynamic toughness was measured by the Kolsky bar technique in which a loading rate of the order of 10^6 MPa $m^{1/2}$ s^{-1} is achieved. Of the three heat treatments employed by them, the one that comes closest to that employed by Ravichandran and Clifton is as follows: austenitize at 845 °C for 1 h, oil quench, and temper at 200 °C for 1 h. Figure 15 shows a fractograph from the room temperature experiments of Chi *et al.* [4]. From the fully dimpled nature of the fracture surface, it can be concluded that failure involved void nucleation and subsequent shear localization. However, in contrast

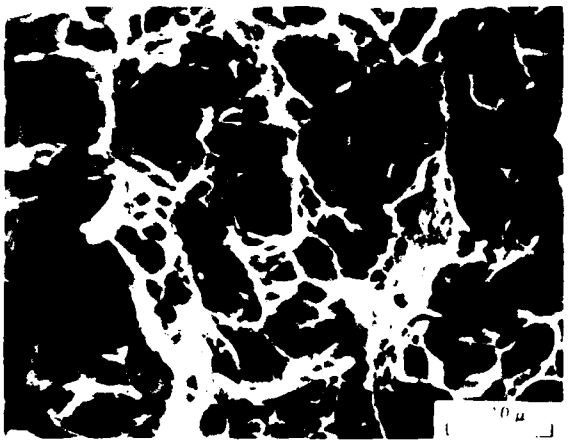

Fig. 15. Fractograph obtained from the work of Chi *et al.* [4] for a room temperature dynamic fracture test.

TABLE 2 Comparison of K_{Ic} data from refs. 1 and 4

Reference	*Fracture toughness* MPa m$^{1/2}$			
	−100 °C		*Room temperature*	
	Static	*Dynamic*	*Static*	*Dynamic*
1	–	32	–	62[a]
4	21	54[b]	46	69[b]

[a] Loading rate $\dot{K}_I = 10^5$ MPa m$^{1/2}$ s^{-1}.
[b] Loading rate $\dot{K}_I = 10^6$ MPa m$^{1/2}$ s^{-1}.

with Figs. 12 and 13, only a small fraction of the fracture surface is covered by the characteristic void sheets resulting from shear localization. Table 2 compares the dynamic fracture toughness obtained in the two works for the low temperature and the room temperature experiments.

Chi *et al.* [4] reported an increase in fracture toughness with an increase in the loading rate. Since the loading rates achieved in the plate impact experiment of Ravichandran and Clifton [1] were about two orders of magnitude higher than those achieved in the Kolsky bar technique used by Chi *et al.* [4], the fracture toughness values obtained in the former work are expected to be higher. However, as seen from Table 2, they are, in fact, lower. In the present work it was established that crack growth occurred in the experiments of Ravichandran and Clifton in a region with approximately 15% upper bainite. Many studies have established that the presence of upper bainite has a deleterious effect on the quasi-static fracture toughness and the impact toughness as measured by the Charpy impact test. Osborne and Embury [18] have shown that the reduced toughness of 4340 steels containing appreciable amounts of upper bainite is related to the morphology of the iron carbides in the bainite. Owing to the high aspect ratio resulting from their stringer-like shape and their relatively large size, these carbides fracture at considerably lower plastic strains and thereby impair toughness. Hence, the discrepancy between the data of Ravichandran and Clifton [1] and of Chi *et al.* [4] can be explained on the basis of the difference in the microstructure of the steels studied in the two works. In particular, it can be argued that the presence of cracked bainitic packets in the near-tip region can promote cleavage fracture of martensite at low temperatures, since the microcracks can serve as cleavage initiation sites for the martensite. On the contrary, the room temperature discrepancy can be explained on two counts.

(a) The presence of 15% upper bainite in the steel used by Ravichandran and Clifton leads to a microstructure in which a fraction (0.15) of the material fails in a brittle manner and thus makes a much reduced contribution to the overall fracture energy.

(b) Judging from the fractograph in Fig. 15, we expect shear localization effects to be present in the room temperature dynamic experiments of Chi *et al.* [4]. However, as evidenced by the smaller fraction of the fracture surface covered by void sheets, the onset of localization is probably delayed in the fully martensitic microstructure. Since failure initiation in the bainitic microstructure occurred by microcracking, whereas in the fully martensitic structure it probably occurred by void nucleation, these observations suggest that microcracks cause the deformation to localize earlier than growing voids because of the greater severity of the strain concentration. Such early localization may curtail the extent of plastic deformation in the martensite prior to fracture and thus reduce the toughness of the microstructure containing a significant fraction of upper bainite.

5. Conclusions

The present work is aimed at understanding the micromechanisms of dynamic crack growth in an AISI 4340 steel studied in the experiments of Ravichandran and Clifton [1]. For this purpose, a fractographic and metallographic examination of

the specimens used by Ravichandran and Clifton in their plate impact experiment was conducted. The observations made in the present work suggest that, for the particular microstructure considered (martensite + 15% upper bainite), the initial stages of failure involve cleavage fracture of bainitic packets in the near-tip region, both at room temperature and at low temperatures. The mode of the subsequent martensitic failure depends on the test temperature. At low temperatures, martensitic failure occurs predominantly by cleavage whereas, at room temperature, it occurs in a ductile manner characterized by localized deformation between the crack tip and the bainitic microcracks.

The present results suggest that the discrepancy between the fracture toughness reported by Ravichandran and Clifton [1] and by Chi *et al.* [4] can be explained on the basis of the difference in the microstructure of the steels studied in the two investigations and that upper bainite has a deleterious effect on both room and low temperature dynamic fracture toughness of 4340 steels.

Acknowledgments

This research was supported by the Army Research Office. Central facilities support was provided through the National Science Foundation Materials Research Group at Brown University.

References

1 G. Ravichandran and R. J. Clifton, *Int. J. Fracture*, in the press.
2 S. Lee, L. Majno and R. J. Asaro, *Metall. Trans. A*, *16* (1985) 1633.
3 Y. Tomita, *Metall. Trans. A*, *18* (1987) 1495.
4 Y. C. Chi, S. H. Lee, K. Cho and J. Duffy, *Tech. Rep. DAAL03-88-K-0015/2*, 1988 (Division of Engineering, Brown University, Providence, RI).
5 G. T. Hahn and A. R. Rosenfield, *Metall. Trans. A*, *6* (1975) 653.
6 E. Smith, T. S. Cook and C. A. Rau, in D. M. R. Taplin (ed.), *Fracture 1977, Proc. 4th Int. Conf. on Fracture*, Vol. 1, University of Waterloo Press, Waterloo, Ontario, 1977, p. 537.
7 R. M. McMeeking, *J. Mech. Phys. Solids*, *16* (1975) 357.
8 D. Pierce, R. J. Asaro and A. Needleman, *Acta Metall.*, *30* (1982) 1087.
9 D. Pierce, R. J. Asaro and A. Needleman, *Acta Metall.*, *12* (1983) 1951.
10 A. Needleman and V. Tvergaard, *J. Mech. Phys. Solids*, *35* (1987) 151.
11 H. Deve, S. Harren, C. McCullough and R. J. Asaro, *Acta Metall.*, *36* (1988) 341.
12 T. B. Cox and J. R. Low, *Metall. Trans. A*, *5* (1974) 1457.
13 T. S. Thomas and A. A. Anctil, *J. Heat Treat.*, *4* (1986) 317.
14 J. H. Giovanola, submitted to *Acta Metall.*
15 M. Azrin, J. G. Cowie and G. B. Olson, *Ann. Isr. Phys. Soc.*, *8* (1986) 409.
16 G. B. Olson, J. F. Mescall and M. Azrin, in M. A. Meyers and L. E. Murr (eds.), *Shock Waves and High-strain-rate Phenomena in Metals: Concepts and Applications*, Plenum, New York, New York, 1981, p. 221.
17 K. M. Cho, Y. C. Chi and J. Duffy, *Tech. Rep. DAAL03-88-K-0015/3*, 1988 (Division of Engineering, Brown University, Providence, RI).
18 D. E. Osborne and J. D. Embury, *Metall. Trans.*, *4* (1973) 2051.